

Topological Phase Transition in a Quasi–Two Dimensional Coulomb Gas

A. Gama Goicochea*

División de Ingeniería Química y Bioquímica, Tecnológico de Estudios Superiores de Ecatepec, Ecatepec de Morelos, Estado de México 55210, Mexico

and

Z. Nussinov

Department of Physics, Washington University, St. Louis, Missouri 63130, USA

Abstract

A system with equal number of positive and negative charges confined in a box with a small but finite thickness is modeled as a function of temperature using mesoscale numerical simulations, for various values of the charges. The Coulomb interaction is used in its three-dimensional form, $U(r) \sim 1 / r$. A topological phase transition is found in this quasi 2d system. The translational order parameter, spatial correlation function, specific heat, and electric current show qualitatively different trends below and above a critical temperature. We find that a 2d logarithmic Coulomb interaction is not essential for the appearance of this transition. This work suggests new experimental tests of our predictions, as well as novel theoretical approaches to probe quasi 2d topological phase transitions.

Keywords: topological phase transition, Kosterlitz-Thouless transition, two dimensional Coulomb gas, dissipative particle dynamics

* Corresponding author. Electronic mail: agama@alumni.stanford.edu

The conventional 2d Coulomb gas consists of logarithmically interacting charges [1–3]. Kosterlitz and Thouless (KT) showed that such a system undergoes a topological phase transition as a function of temperature [1]. As the system is heated, a transition appears between its low temperature dielectric phase and a conducting high temperature phase [1]. The transition temperature is $T_{KT}^* = q^{*2}/4$, where q^* is the charge, in the low density limit [4]. Asterisked symbols represent adimensional quantities. The properties of the 2d Coulomb gas have been studied theoretically [1–8] and with numerical simulations [9–17]. At temperatures below T_{KT}^* , correlations drop algebraically with distance, with a temperature dependent exponent. By contrast, at temperatures above T_{KT}^* , the correlations decay exponentially [1]. The KT transition has long been viewed as the quintessential “topological phase transition” that occurs despite the absence of a well-defined local order parameter (forbidden by the Mermin–Wagner–Coleman theorem [18]). Here, at finite temperature, no continuous symmetry breaking occurs. However, at temperatures $T^* < T_{KT}^*$, the correlations can become very long ranged displaying the said algebraic decay with distance. Topological transitions also appear in gauge theories that model fundamental interactions. By Elitzur’s theorem [19] no local order parameter can appear since gauge symmetry may not be broken. The latter transitions in gauge theories are typically discontinuous (first order) or conventional continuous (i.e., second order) transitions [20, 21]. Both KT transitions and phase transitions in gauge theories occur from a confined phase (of particles or topological defects, such as vortices or other excitations) to a deconfined phase. The KT transition is unique in various ways. Perhaps most strikingly, it is neither a conventional first nor second order transition but is rather an endpoint of a continuous line of critical points. Along this critical line, at $T^* < T_{KT}^*$, the system exhibits the above noted KT algebraic decay of correlations. There are other 2d systems that undergo KT type transitions, of which we note only a few. These include

point charges [22], a solid with dislocations [23] and perhaps most well-known, the XY spin model (including recent experimental observation in magnetic crystalline materials [24]) and superfluid films [25]. It also appears in thin superconducting films where the interaction between vortices is logarithmic at short range [26]. KT transitions are ubiquitous to $p > 5$ state 2d classical clock models [27] and related 1d clock models [28] and feature prominently in quantum spin chains and 2d quantum dimer models [29, 30]. Typically, in one form or another, all equilibrated systems that display a KT transition can be mapped onto an effective 2d plasma of interacting charges. However, with the exception of gauge theories, all of the above noted studies were carried out for strictly 2d systems. Indeed, excusing Renormalization Group considerations for finite thickness systems and the investigation of truly higher dimensional driven non-equilibrium XY models featuring KT-type transitions [31], the detailed nature of the transitions in equilibrated quasi-2d systems (in particular, those in hard/soft sphere charged fluids that form the focus of our work [5, 32]) has long remained largely unexplored.

Here we study a low density, quasi – 2d Coulomb gas of spheres confined to move in a box whose thickness is small but finite, by means of numerical simulations. The specific query that motivated our study is that of determining how the topological transition of pristine 2d systems evolves as these acquire a thickness in a transverse direction [33]. That is, what transpires when instead of having charges (either exact or effective, e.g., vortices or dislocations) interacting via 2d, logarithmic-type interactions, the system is a thin layer, and the particles are 3d spheres? In investigating this question, we found that various features persist. Our results may afford a more direct comparison with experiments—which are not truly 2d [34–36]. The large-distance electrostatic interaction that we focus on is, accordingly, modeled as the typical 3d electrostatic interactions, $U(r) \sim 1 / r$ where r is the relative distance separating the charges, instead of

$U(r) \sim \ln(1/r)$ for strictly 2d systems. These systems are neutral, with an equal number of positively and negatively charged particles. For the non-electrostatic interactions, we use the dissipative particle dynamics (DPD) model [37, 38], which is driven by conservative, dissipative, and random forces. The latter forces are short ranged, repulsive and pairwise additive. The conservative force is given by $\vec{F}_{ij}^C(r_{ij}^*) = a_{ij}^*(1 - r_{ij}^*/r_c^*)\Theta(r_c^* - r_{ij}^*)\hat{r}_{ij}$, where a_{ij}^* is the intensity of the force, which is chosen here as $a_{ij}^* = 78.3$ in dimensionless units [39]. Although this type of force allows for some overlap of the particles, our choice of a_{ij}^* reduces it [40]. The length $r_c^* = 1$ is a cutoff radius and $\Theta(x)$ is the Heaviside step function. The dissipative and random forces are, respectively, given by $\vec{F}_{ij}^D(r_{ij}^*) = -\gamma(1 - r_{ij}^*/r_c^*)^2[\hat{r}_{ij} \cdot \vec{v}_{ij}^*]\Theta(r_c^* - r_{ij}^*)\hat{r}_{ij}$ and $\vec{F}_{ij}^R(r_{ij}^*) = \sigma(1 - r_{ij}^*/r_c^*)\Theta(r_c^* - r_{ij}^*)\xi_{ij}\hat{r}_{ij}$, [38]. Here, $\vec{v}_{ij}^* = \vec{v}_i^* - \vec{v}_j^*$ is the relative velocity between particles i and j . Due to the fluctuation-dissipation theorem, $\sigma^2/2\gamma = k_B T$, where k_B is Boltzmann's constant and T is the absolute temperature [38]. The amplitudes ξ_{ij} are randomly drawn from a uniform distribution between 0 and 1. To confine the charges so that they move on a thin slit, an effective wall force is applied at both ends of the simulation box along the z -direction, given by $\vec{F}_{wall}(z^*) = a_w^*(1 - z^*/z_c^*)\Theta(z_c^* - z^*)\hat{z}$ [41]. The prefactor a_w^* sets the maximal size of this wall strength that has z_c^* as its cutoff distance. The role of this featureless wall force is only to confine the motion of the charges on a slit. The charges are modeled as charge distributions centered at the center of mass of each particle, given by $\rho_{q^*}(r^*) = (q^*/\pi\lambda^{*3})\exp(-2r^*/\lambda^*)$ [42, 43]. Here, λ^* is the decay length of the charge distribution and q^* is the total charge carried by the particle. It has been shown [43] that for $r^* \leq r_c^*$ (the particles' radius), the electrostatic force between these charge distributions tends to zero as $r \rightarrow 0$. For $r^* > r_c^*$ the electrostatic potential assumes its usual form, $U(r) \sim 1/r$, and its long range contribution

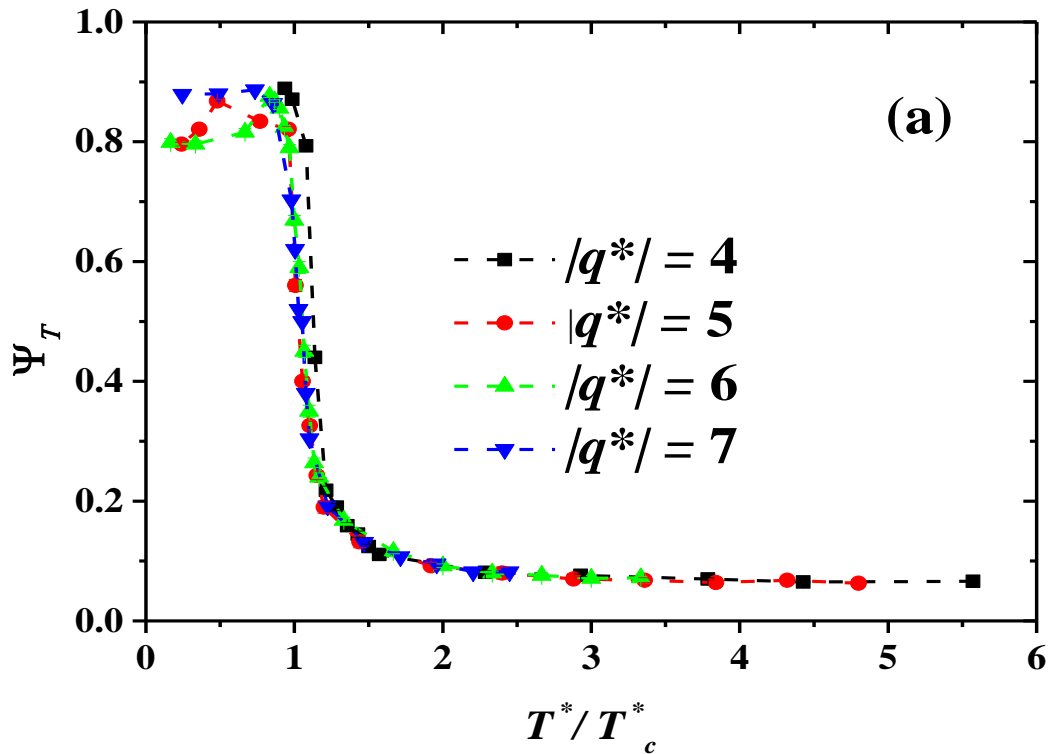
is calculated using the Ewald sums [44]. Using this charge model with the conservative DPD force, the collapse of particles with opposite charge is avoided, and no singularity occurs in the Coulomb interaction at the shortest distances. The number density, defined as the total number of charged particles N divided by the volume of the simulation box V , is in all cases equal to $\rho^* = 0.03$. The thickness of the simulation box is fixed at $L_z^* = 1$ while its square transversal area depends on the total number of charged particles, which goes from $N = 200$, up to 3×10^4 . The simulations are run for up to 4×10^3 blocks of $10^3 \delta t^*$ each, with the time step set at $\delta t^* = 0.01$. Periodic boundary conditions are applied along the x - and y - axes but not along the z -direction since the walls are impenetrable. Full details about the method, algorithm and other details have been published elsewhere [40, 41, 43].

To track the phase transition, we calculate the translational order parameter (TOP) of the particles, defined as follows [44]:

$$\Psi_T = \frac{1}{N} \left\langle \left| \sum_{j=1}^N e^{i\vec{K} \cdot \vec{r}_j^*} \right| \right\rangle, \quad (1)$$

where N is the total number of particles, and \vec{K} is the first shell reciprocal lattice vector. The angular brackets denote an average over time. Figure 1(a) shows the dependence of TOP on temperature for increasing values of the charge. We find a transition from an ordered low temperature state to a disordered high temperature state, as shown in Fig. 1. The associated transition temperature T_c^* monotonically increases with the magnitude of the charge $|q^*|$. Interestingly, *on scaling the temperature by $T_c^* = q^{*2}/4$, all of the TOP curves collapse into a single universal function*, (Fig. 1(a)). The TOP is approximately constant below T_c^* , where the charges are all paired, and it decays sharply at temperatures above T_c^* . Although the TOP depends on the size of the system, becoming smaller as the size increases, T_c^* does not scale with the system size (see Fig. 1(b), for $|q^*| = 7$). At the

onset of the transition, the cluster formed by the grouping of dipoles begins to dissociate, fragmenting into smaller groups of dipoles [10, 11]. This splintering causes the TOP to decrease rapidly with a small rise of the temperature, reaching a plateau. At the highest temperatures, some charges still appear in isolated dipoles. The TOP is small but remains non-zero at those temperatures. For sufficiently large systems, several clusters of dipolar pairs are formed, giving rise to a phase with algebraic order only. When extrapolated to the thermodynamic limit, our data suggest that the TOP tends to zero, as expected for a topological phase transition having no local order parameter. For a fixed value of the single particle charge, so long as the system remains globally neutral and confined along the z -direction, the transition between a state where all charges are bound to one where they are unbound occurs at the same temperature.



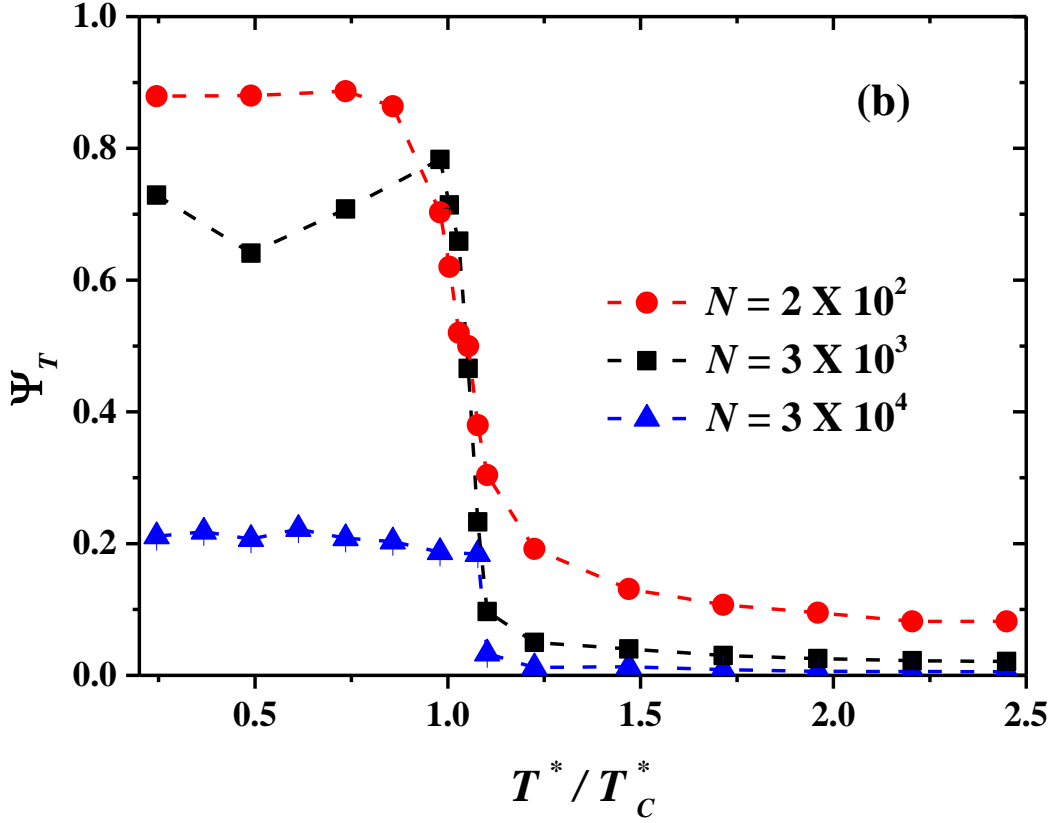


Figure 1. (a) The translational order parameter Ψ_T as a function of the scaled temperature, T^*/T_C^* for four values of the charge on the particles. In all cases, $\rho^* = 0.03$, $N = 200$; error bars are smaller than the symbol's size. The dashed lines are guides for the eye. (b) Ψ_T as a function of the scaled temperature at fixed number density $\rho^* = 0.03$ and charge $|q^*| = 7$ as the total number of charged particles N is increased.

The radial distribution function (RDF), $g(r)$, for particles of opposite charge is shown in Fig. 2, at $T^* < T_C^*$ (Figs 2(a) and (b)), and at $T^* > T_C^*$ (Figs. 2(c) and (d)). At the lowest temperatures, all dipoles are bound in dipole pairs, see Fig. 2(b). The sharp maxima displayed at relatively short distances in the RDF (Fig. 2(a)) correspond to closely bound dipolar pairs [15]. Accordingly, maxima appear at $r^* = 1, \sqrt{5}, \sqrt{8}, \dots$, etc., as a consequence of the coordination of opposite charges forming a square lattice on the xy -plane, with the first peak due to dipolar pairs, the second to four-charge clusters, and so on. The long-range behavior of the RDF, indicated by the dashed line in Fig. 2(a), shows algebraic decay, as expected [1–4]. To capture this dependence, the area of the simulation

box has to be large enough to allow for the formation of dipolar clusters. If the number of charges is small, they all condense into a single square lattice at the lowest temperature. The snapshot in Fig. 2(b) shows all charges condensed into clusters with quasi-long range order at the lowest temperature. At $T^* > T_c^*$, the RDF decays exponentially [1–3], see Fig. 2(c). The charge clusters are dissolved, and most charges move individually, although some remain bound in dipoles; see Fig. 2(d). Comparison of the RDFs below (Fig. 2(a)) and above (Fig. 2(c)) T_c^* vividly sheds light on the nature of this phase transition [1]. Most of the structure of the system when it is condensed, at $T^* < T_c^*$ (Figs. 2(a), (b)) vanishes at $T > T_c^*$ (Figs. 2(c), (d)).

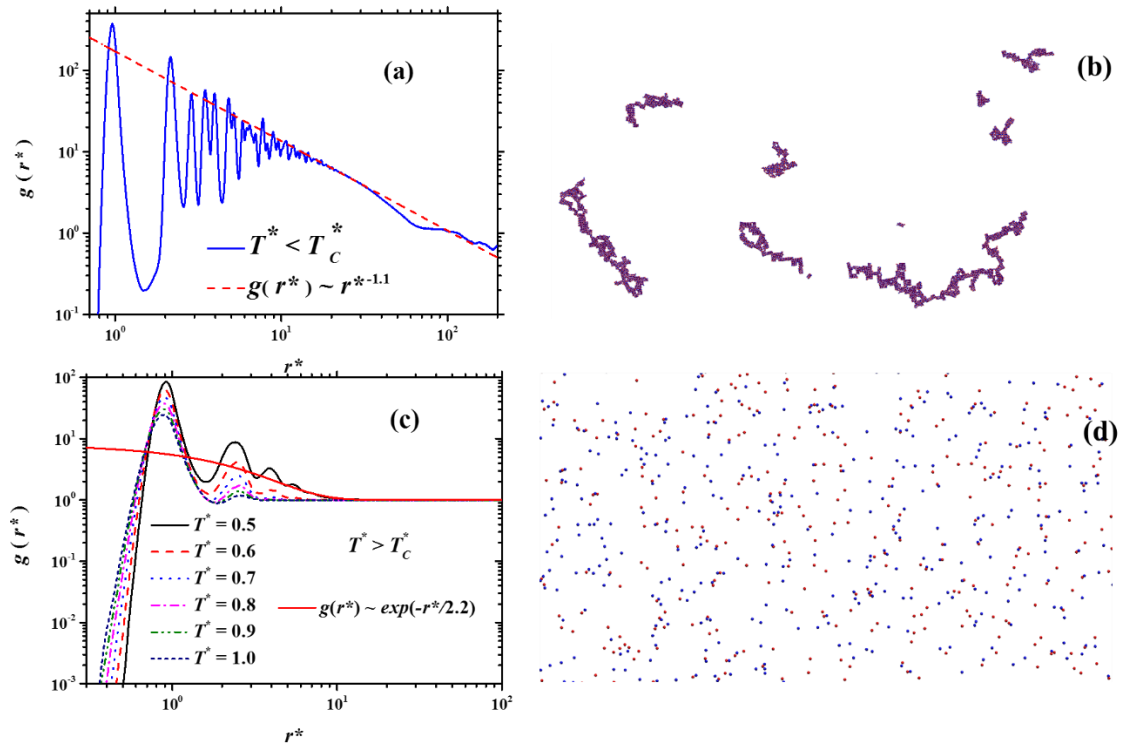


Figure 2. (a) The RDF and (b) snapshot of oppositely charged spheres at $T^* = 0.1 < T_c^*$. The RDFs shown in (c) are all for $T^* > T_c^*$, with $T_c^* = 0.41$. The snapshot in (d) shows the system at $T^* = 1.0$. The dashed red line in (a) is the fit to the function $g(r^*) \sim r^{*-\eta}$, with $\eta = 1.1$. The solid red line in (c) is the function $g(r^*) \sim \exp(-r^*/2.2)$. The snapshot in (d) is taken at $T^* = 1.0 > T_c^*$, showing most charges unpaired. Red/blue circles are positive/negative charges. In all cases, $\rho^* = 0.03$, $|q^*| = 7$, $N = 3 \times 10^4$. The snapshots were obtained with VMD [45].

In Fig. 3(a) we show the evolution of the density of free charges with increasing temperature for two values of the charge. The charges are considered free if their relative distance is $r_{ij}^* \geq 1.4$. As Fig.3(a) shows, the number of free charges increases rapidly as the temperature grows above T_C^* , following the same trend for both values of the charge on each sphere. The solid line in Fig. 3(a) corresponds to the approximate analytical solution, provided by Minnhagen [3] for the Kosterlitz – Thouless transition in charged disks. It is concluded that the quasi 2d condensed phase melts similarly as the strictly 2d phase does. At temperatures below the transition temperature, the spatial correlations between charges of opposite sign decay as a power law, $g(r_{ij}^*) \sim 1/r_{ij}^{*\eta}$, where the exponent η depends linearly on temperature, for T^* well below T_C^* ; see Fig. 3(b). This is in agreement with the expected behavior for the strictly 2d KT transition [1]. At T_C^* , $\eta \approx 4.5 \pm 1.8$, which is much larger than the expected value for the KT transition, $\eta = 1/4$ [1]. A more appropriate comparison would be with the value of the exponent extrapolated from the low temperature data (black line in Fig. 3(b)), where the power law dependence of $g(r_{ij}^*)$ is well defined. There, one finds $\eta = 2.1$. Although notably larger than the expected 2d value, this value of η is not too different from that found in other, quasi – 2d models [46, 47].

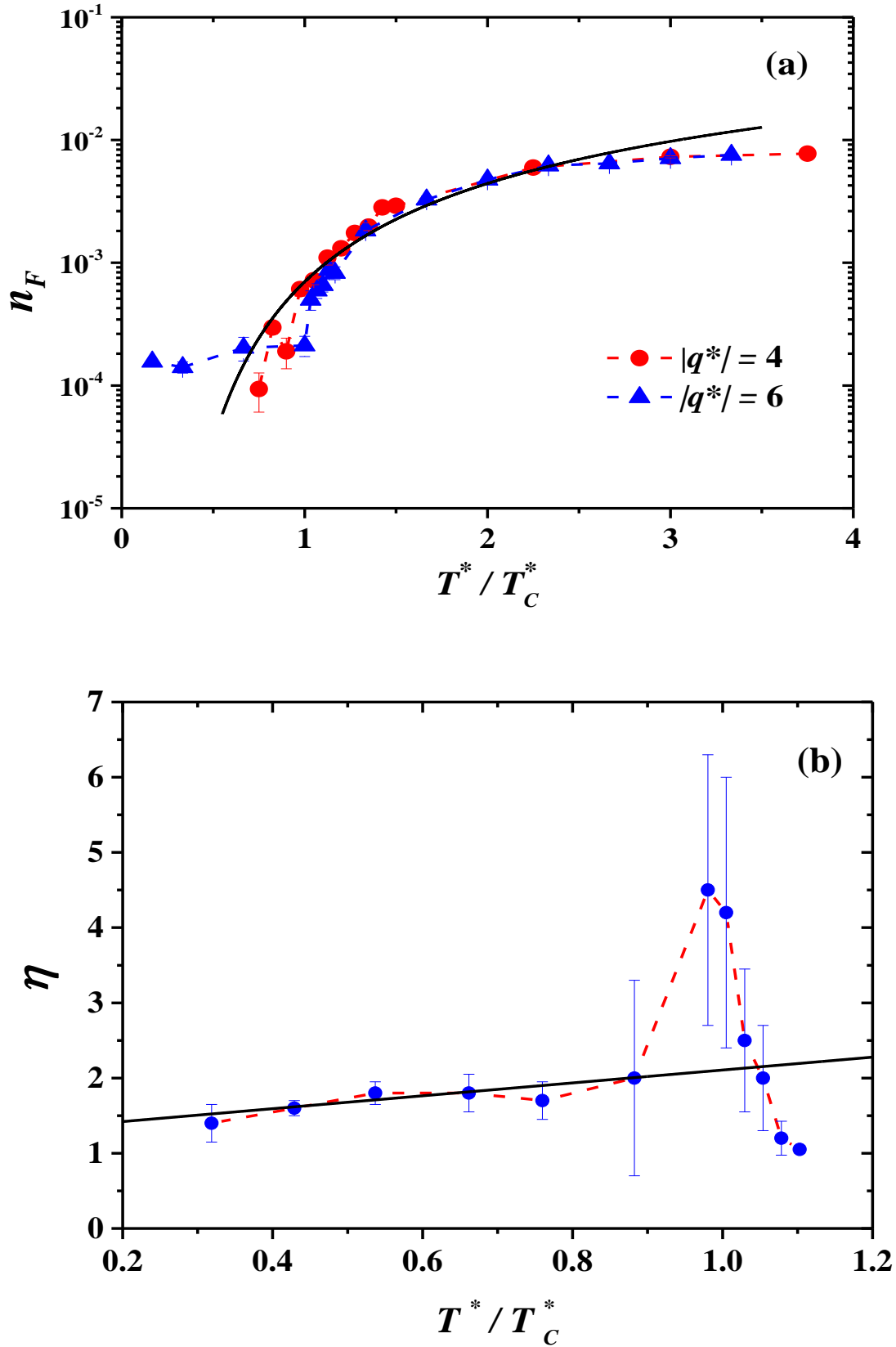


Figure 3. (a) Density of free charged spheres, n_F , regardless of their sign, as a function of reduced temperature for spheres with charge $|q^*| = 4$ (red circles) and $|q^*| = 6$ (blue triangles). In both cases there are $N = 200$ charged particles, with total number density

$\rho^* = 0.03$. The solid black line represents an approximate analytical solution for finite screening length of the Coulomb interaction between disks taken from [3]. (b) Exponent (η) of the algebraic decay of the radial distribution function between charges of opposite sign, $g(r_{ij}^*) \sim 1/r_{ij}^{*\eta}$, as a function of the normalized temperature. The solid black line is the best linear fit for the data below T_c^* . There are 3×10^4 particles in the system with $|q^*| = 7$ and $\rho^* = 0.03$.

The transition found here can be understood as being driven by the proliferation of defects that melt the crystal [1, 48, 49]. As shown by Toxvaerd [50], the lattice melts as the temperature increases, where the defects become charge quadruplets or disclinations. The role of disclinations is played by dipolar pairs. We calculate the specific heat, $C_V^* = 1/Nq^{*2} (\partial U^* / \partial T^*)_V$, as $|q^*|$ increases, from numerical differentiation of the total internal energy curves, U^* . As seen in Fig. 4, we find that C_V^* has a maximum at $T^* \sim T_c^*$, regardless of the charge, in agreement with previous reports for strictly 2d systems [9, 11–13, 15, 17]. The maximum in C_V^* occurs at a temperature that increases with $|q^*|$, since larger energy is required to unbind dipoles for larger charge and becomes smaller in magnitude as $|q^*|$ increases. The stronger coupling produced by increasing $|q^*|$ makes the transition broader, with more dipolar pairs present at $T^* > T_c^*$. This behavior reproduces that found for C_V^* of charged disks below and above T_c^* [15]. Once T^* is renormalized by the corresponding T_c^* for each charge, the maximum in C_V^* occurs at roughly the same normalized temperature, for all the values of q^* ; see Fig. 4.

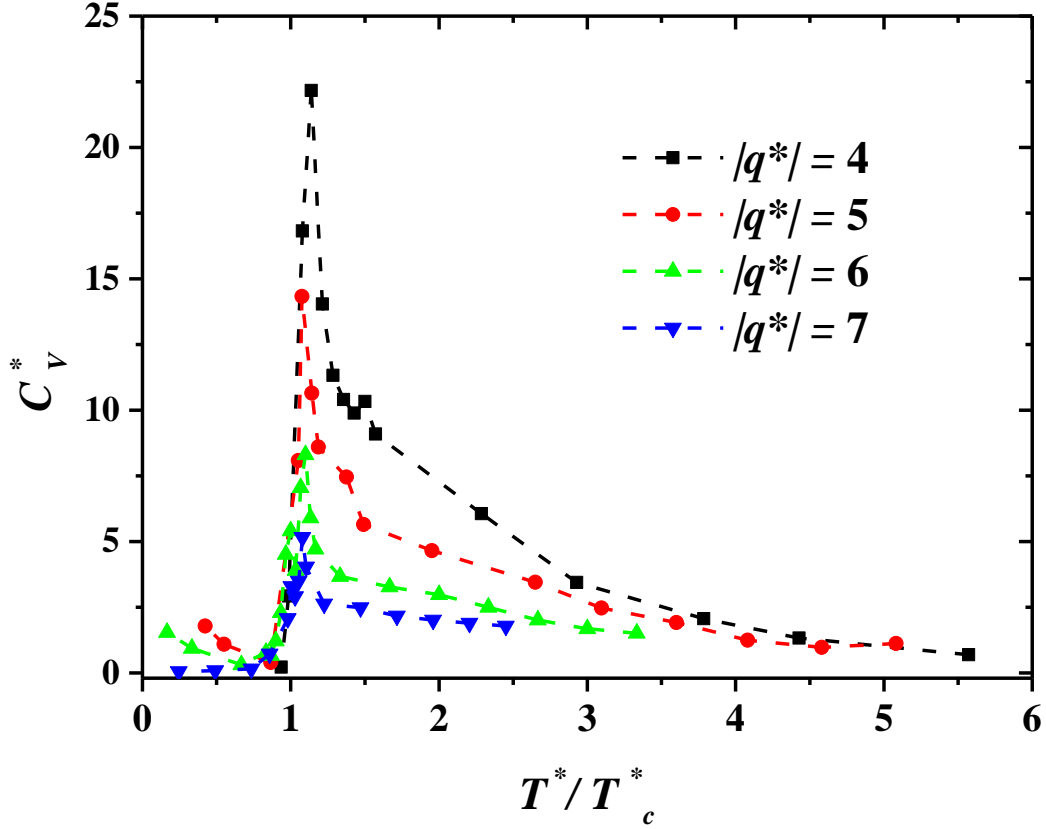


Figure 4. Specific heat, $C_V^* = 1/Nq^{*2} (\partial U^*/\partial T^*)_V$, as a function of temperature normalized by T_c^* , for four values of the charge. In all cases, $\rho^* = 0.03$, $N = 200$ and the error bars are smaller than the symbols' size. The dashed lines are guides for the eye.

Lastly, we calculate the average current in the system, I_x^* , once a weak electric field $\vec{E}^* = 0.02\hat{x}$ is applied along the x -axis of the simulation box, for particles with charge $|q^*| = 5$. The current is given by

$$I_x^* = \frac{1}{Nr_c^*} \langle |\sum_{i=1}^N q_i^* \vec{v}_{ix}^*| \rangle, \quad (2)$$

where \vec{v}_{ix}^* is the x -component of the velocity of the i -th particle with charge q_i^* , and $r_c^* = 1$ is the cutoff length of the non-electrostatic forces. The results are shown in Fig. 5, where U^* is included also, for comparison. There is clearly a transition from a low temperature dielectric phase to a conducting phase at $T^* > T_c^*$, as in the strictly 2d KT transition. Consistent with Ohm's law, the temperature dependence of the current follows

that of U^* . The inset in Fig. 5 presents U^* vs I_x^* , where a linear dependence between them clearly arises. The trends found in both C_V^* (Fig 5) and U^* (Fig. 5) are the same as those found for charged disks in strictly 2d systems [9, 14].

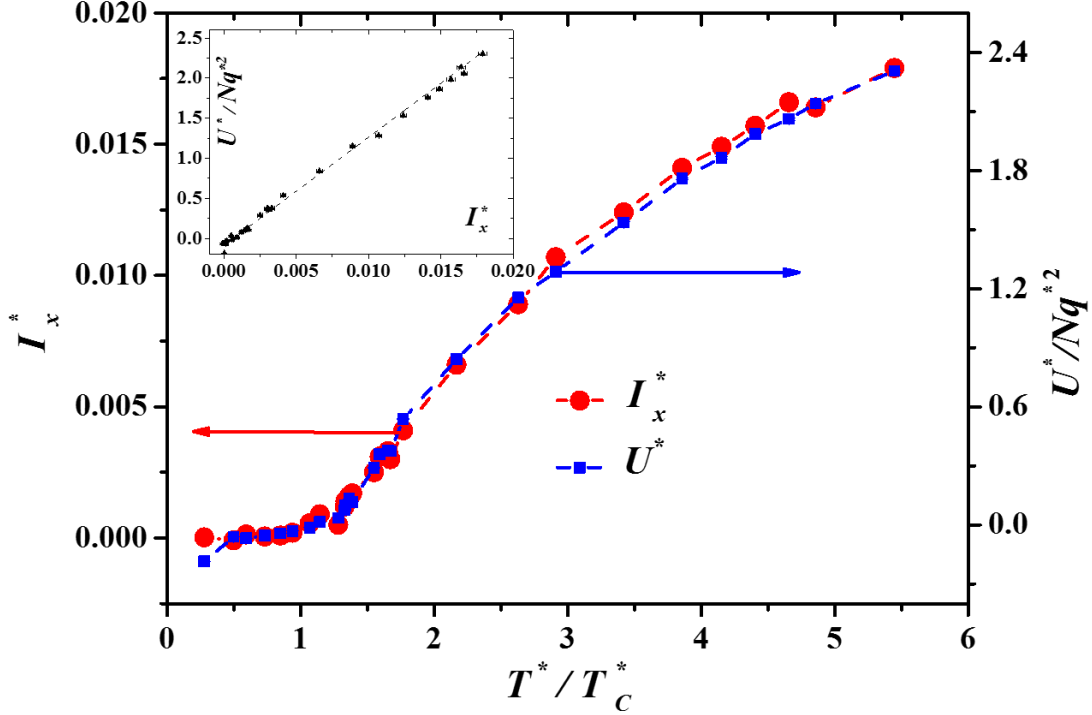


Figure 5. Comparison of the internal energy, U^*/Nq^{*2} , (blue squares, right axis) with the average current along the direction of the applied electric field, I_x^* , (red circles, left axis), when $E^* = 0.02$ is applied along the x axis. The dashed lines joining the data are guides for the eye. The inset shows the dependence of U^*/Nq^{*2} on I_x^* ; the dashed line is the best linear fit. For all curves, $\rho^* = 0.03$, $N = 200$, $|q^*| = 5$ and the error bars are smaller than the symbol sizes.

The phase transition found here may, once again, be understood as being driven by a proliferation of defects in the form of pairs of opposite charges that melt the crystal. At the onset of the melting transition bound dislocation pairs begin to appear. Raising the temperature leads to the appearance of more dislocations and disclinations, with some remaining at the largest temperature modeled here. This scenario is similar to the KTHNY theory [1, 48, 49] that predicts that the 2d crystal melts due to the unbinding of dislocations and the spread of disclinations. Consequently, the effective interactions between defects responsible for the phase transition in this quasi-2d system may be

predominantly logarithmic, as they are in the KTHNY theory, although the electrostatic pair interactions vary as $1/r$.

To summarize, the structural, thermodynamic, and dynamic properties of neutral systems of charged spheres confined to move in a quasi-2d geometry have been obtained at various temperatures, for various charge values. We find that it is possible to locate a topological phase transition in a low density Coulomb gas that is not strictly confined to 2d but has a finite thickness, and that its properties resemble those of its strictly 2d counterpart. The T_c^* is found to take place at $T_c^* = q^{*2}/4$, as predicted for disks [1–8]. The explicit dependence of the Coulomb interaction ($\ln(r)$ or $1/r$) is not crucial for the appearance of the topological phase transition but charge neutrality in reduced dimensionality is [11]. This is relevant for comparison with, understanding of and interpretation of recent quasi-2d experiments. Our approach may suggest new experimental tests of our predictions, such as in colloids trapped between membranes, as well as new theoretical approaches to probe this type of topological phase transition.

ACKNOWLEDGEMENTS

AGG acknowledges J. D. Hernández–Velázquez for enlightening discussions, and the computer resources offered by the Laboratorio de Supercómputo y Visualización en Paralelo (LSVP – Yoltla) of UAM – Iztapalapa, where the simulations were carried out.

REFERENCES

- [1] J. M. Kosterlitz, D. J. Thouless, “Ordering, metastability and phase transitions in two-dimensional systems”, *J. Phys. C: Solid State Phys.* **6**, 1181 (1973).
- [2] J. M. Kosterlitz, “Kosterlitz–Thouless physics: a review of key issues”, *Rep. Prog. Phys.* **79**, 026001 (2016).

- [3] P. Minnhagen, “The two-dimensional Coulomb gas, vortex unbinding, and superfluid-superconducting films”, *Rev. Mod. Phys.* **59**, 1001 (1987).
- [4] J. S. Høye, K. Olaussen, “The two-dimensional Coulomb gas in the critical region”, *Physica* **107A**, 241 (1981).
- [5] Y. Levin, X. – J. Li, M. E. Fisher, “Coulombic Criticality in General Dimensions”, *Phys. Rev. Lett.* **73**, 2716 (1994).
- [6] L. Šamaj, *J. Phys. A: Math. Gen.* **36**, 5913 (2003).
- [7] J. Fröhlich, T. Spencer, “Kosterlitz-Thouless transition in the two-dimensional plane rotator and Coulomb gas”, *Phys. Rev. Lett.* **46**, 1006 (1981).
- [8] B. Cichocki, B. U. Felderhof, “Electrostatic interactions in two-dimensional Coulomb systems with periodic boundary conditions”, *Physica A* **158**, 706 (1989).
- [9] Y. Saito, H. Müller–Krumbhaar, “Two-dimensional Coulomb gas: A Monte carlo study”, *Phys. Rev. B* **23**, 308 (1981).
- [10] G. Orkoulas, A. Z. Panagiotopoulos, “Phase diagram of the two-dimensional Coulomb gas: A thermodynamic scaling Monte Carlo study”, *J. Chem. Phys.* **104**, 7205 (1996).
- [11] E. Lomba, J. J. Weis, F. Lado, “Structure and thermodynamics of a two-dimensional Coulomb fluid in the strong association regime”, *J. Chem. Phys.* **127**, 074501 (2007).
- [12] J. M. Caillol, D. Levesque, “Low-density phase diagram of the two-dimensional Coulomb gas”, *Phys. Rev. B* **33**, 499 (1986).
- [13] J. Aupic, T. Urbic, “A structural study of a two-dimensional electrolyte by Monte Carlo simulations”, *J. Chem. Phys.* **142**, 014506 (2015).
- [14] J. Clerouin, J.-P. Hansen, “Delocalization Transition of a Classical Two-Dimensional Coulomb Lattice”, *Phys. Rev. Lett.* **54**, 2277 (1985).
- [15] J. Clerouin, J.-P. Hansen, B. Piller, “Two-dimensional classical electron gas in a periodic field: Delocalization and dielectric-plasma transition”, *Phys. Rev. A* **36**, 2793 (1987).
- [16] A. Alastuey, F. Cornu, B. Jancovici, “Comment on “Two-dimensional classical electron gas in a periodic field: Delocalization and dielectric-plasma transition””, *Phys. Rev. A* **38**, 4916 (1988).
- [17] J. Lidmar, M. Wallin, “Monte Carlo simulations of a two-dimensional continuum Coulomb gas”, *Phys. Rev. B* **55**, 522 (1997).
- [18] M. D. Mermin, H. Wagner, “Absence of ferromagnetism or antiferromagnetism in one-or two-dimensional isotropic Heisenberg models”, *Phys. Rev. Lett.* **17**, 1133 (1966).
S. Coleman, “There are no Goldstone bosons in two dimensions”, *Commun. Math. Phys.* **31**, 259 (1973).
- [19] S. Elitzur, “Impossibility of spontaneously breaking local symmetries”, *Phys. Rev. D* **12**, 3978 (1975).

- [20] J. B. Kogut, “An introduction to lattice gauge theory and spin systems”, *Rev. Mod. Phys.* **51**, 659, (1979).
- [21] M. C. Ogilvie, “Phases of gauge theories”, *J. Phys. A: Math. Theor.* **45**, 483001 (2012).
- [22] J. P. Hansen, P. Viot, “Two-body correlations and pair formation in the two-dimensional Coulomb gas”, *J. Stat. Phys.* **38**, 823 (1985).
- [23] M. A. Bates, D. Frenkel, “Influence of vacancies on the melting transition of hard disks in two dimensions”, *Phys. Rev. E* **61**, 5223 (2000).
- [24] Z. Hu et al., “Evidence of the Berezinskii-Kosterlitz-Thouless phase in a frustrated magnet”, *Nat. Commun.* **11**, 5631 (2020).
- [25] D. J. Bishop, J. D. Reppy, “Study of the Superfluid Transition in Two-Dimensional ^4He Films”, *Phys. Rev. Lett.* **40**, 1727 (1978).
- [26] V. G. Kogan, “Interaction of vortices in thin superconducting films and the Berezinskii-Kosterlitz-Thouless transition”, *Phys. Rev. B* **75**, 064514 (2007).
- [27] T. Surungan, et al., “Berezinskii–Kosterlitz–Thouless transition on regular and Villain types of q-state clock models”, *J. Phys. A: Math. Theor.* **52**, 275002 (2019).
- [28] G. Sun et al., “Phase transitions in the Z_p and U(1) clock models”, *Phys. Rev. B* **100**, 094428 (2019).
- [29] C. Castelnovo et al., “Zero-temperature Kosterlitz–Thouless transition in a two-dimensional quantum system”, *Ann. Phys.* **322**, 903 (2007).
- [30] F. S. Nogueira, Z. Nussinov, “Renormalization, duality, and phase transitions in two- and three-dimensional quantum dimer models”, *Phys. Rev. B* **80**, 104413 (2009).
- [31] T. Haga, “Nonequilibrium Kosterlitz-Thouless transition in a three-dimensional driven disordered system”, *Phys. Rev. E* **98**, 032122 (2018).
- [32] J. J. Weis, D. Levesque, J. M. Caillol, “Restricted primitive model of an ionic solution confined to a plane”, *J. Chem. Phys.* **109**, 7486 (1988).
- [33] M. Mazars, “Long ranged interactions in computer simulations and for quasi-2D systems”, *Phys. Rep.* **500**, 43 (2011).
- [34] A. Ashoka, K. S. Bhagyashree, and S. V. Bhat, “Signatures of field-induced Berezinskii-Kosterlitz-Thouless correlations in the three-dimensional manganite $\text{Bi}_{0.5}\text{Sr}_{0.5}\text{Mn}_{0.9}\text{Cr}_{0.1}\text{O}_3$ ”, *Phys. Rev. B* **102**, 024429 (2020).
- [35] Y. Togawa, et al., “Formations of Narrow Stripes and Vortex–Antivortex Pairs in a Quasi-Two-Dimensional Ferromagnet K_2CuF_4 ”, *J. Phys. Soc. Jpn.* **90**, 014702 (2021).
- [36] L. Meng et al., “Anomalous thickness dependence of Curie temperature in air-stable two-dimensional ferromagnetic 1T-CrTe_2 grown by chemical vapor deposition”, *Nat. Commun.* **12**, 809 (2021).

- [37] P. J. Hoogerbrugge, J. M. V. A. Koelman, “Simulating Microscopic Hydrodynamic Phenomena with Dissipative Particle Dynamics”, *Europhys. Lett.* **19**, 155 (1992).
- [38] P. Español, P. Warren, “Statistical mechanics of dissipative particle dynamics”, *Europhys. Lett.*, **30**, 191 (1995).
- [39] I. V. Pivkin, G. E. Karniadakis, “Coarse-graining limits in open and wall-bounded dissipative particle dynamics systems”, *J. Chem. Phys.* **124**, 184101 (2006).
- [40] K. A. Terrón–Mejía, R. López–Rendón, A. Gama Goicochea, “Electrostatics in dissipative particle dynamics using Ewald sums with point charges”, *J. Phys. Cond. Matt.* **28**, 425101 (2016).
- [41] A. Gama Goicochea, “Adsorption and disjoining pressure isotherms of confined polymers using dissipative particle dynamics”, *Langmuir* **23**, 11656 (2007).
- [42] R. D. Groot, “Electrostatic interactions in dissipative particle dynamics—simulation of polyelectrolytes and anionic surfactants”, *J. Chem. Phys.* **118**, 11265 (2003).
- [43] M. González-Melchor, E. Mayoral, M. E. Velázquez, J. Alejandre, “Electrostatic interactions in dissipative particle dynamics using the Ewald sums”, *J. Chem. Phys.* **125**, 224107 (2006).
- [44] M. P. Allen, D. J. Tildesley, *Computer Simulation of Molecular Liquids*; Oxford University Press. Oxford, 1987.
- [45] W. Humphrey, A. Dalke, K. Schulten, “VMD: visual molecular dynamics”, *J. Molec. Graphics* **14**, 33 (1996).
- [46] H. Kleinert, F. S. Nogueira, A. Subdø, “Kosterlitz–Thouless-like deconfinement mechanism in the (2+1)-dimensional Abelian Higgs model”, *Nuclear Phys. B* **666**, 361 (2003).
- [47] V. Shyta, J. van den Brink, F. S. Nogueira, “Deconfined Criticality and Bosonization Duality in Easy-Plane Chern-Simons Two-Dimensional Antiferromagnets”, *Phys. Rev. Lett.* **127**, 045701 (2021).
- [48] D. R. Nelson, B. I. Halperin, “Dislocation-mediated melting in two dimensions”, *Phys. Rev. B* **19**, 2457 (1979).
- [49] A. P. Young, “Melting and the vector Coulomb gas in two dimensions”, *Phys. Rev. B* **19** 1855 (1979).
- [50] S. Toxvaerd, “Computer simulation of melting in a two-dimensional Lennard-Jones system”, *Phys. Rev. A* **24**, 2735 (1981).